

Supporting information

High-quality perovskite films prepared by nucleus epitaxial growth for efficient and stable perovskite solar cells

Tiao Wu^a, Wenxi Ji^b, Longgui Zhang^b, Qiaoyun Chen^a, Jianfei Fu^a, Jiajia Zhang^a, Zelong Zhang^a, Yi Zhou^{a,*}, Bin Dong^a, Bo Song^{a,*}

^a *Laboratory of Advanced Optoelectronic Materials, Suzhou Key Laboratory of Novel Semiconductor-optoelectronics Materials and Devices, College of Chemistry, Chemical Engineering and Materials Science, Soochow University, Suzhou 215123, China*

^b *Beijing Research Institute of Chemical Industry China Petroleum & Chemical Corporation, Beijing 100013, PR China*

Tel. : +86 (0) 512 65882507; *E-mail:* yizhou@suda.edu.cn; songbo@suda.edu.cn

Table S1. Comparison of our device with published perovskite solar cells.

Perovskite composition	Nucleus composition	w/o nucleus	PCE w nucleus	Ref.
FA _{0.98} MA _{0.02} PbI ₃	δ-FAPbI ₃	21.53%	23.16%	This work
(FAPbI ₃) _{1-x} (MAPbBr ₃) _x	δ-CsPbI ₃	19.16%	20.45%	¹
FA _{0.91} MA _{0.09} Pb(I _{0.91} Br _{0.09})	δ-CsPbI ₃ /δ-RbPbI ₃	20.42%	22.30%	²
Cs _{0.05} FA _{0.95} PbI ₃	CsPbBr ₃	20.30%	21.45%	³
FA _{0.98} MA _{0.02} PbI ₃	δ-CsPbI ₂ Br	20.61%	21.63%	⁴
(FAPbI ₃) _{0.96} (MAPb ₃) _{0.04}	Cs _{0.1} FA _{0.78} MA _{0.12} Pb _{2.55} Br _{0.45}	19.4%	21.7%	⁵
FA _{0.75} MA _{0.25} PbI ₃	(BDA)PbI ₄	21.03%	23.95%	⁶

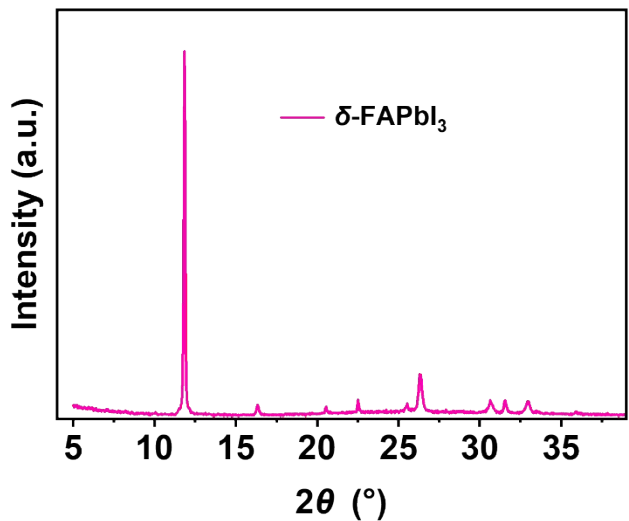


Figure S1. XRD patterns of δ -FAPbI₃.

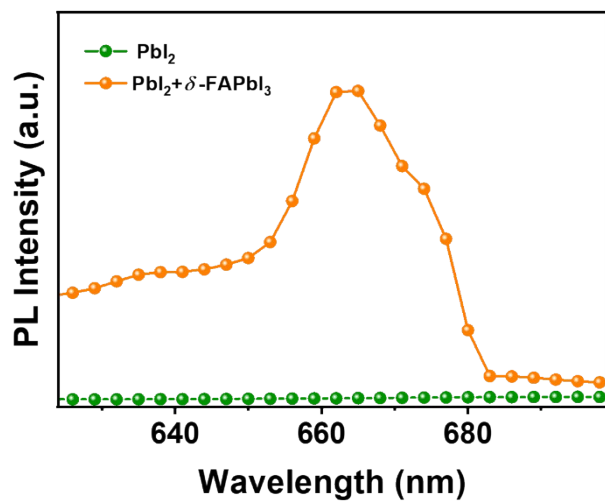


Figure S2. Steady-state PL spectra of PbI₂ and PbI₂ + δ -FAPbI₃ films.

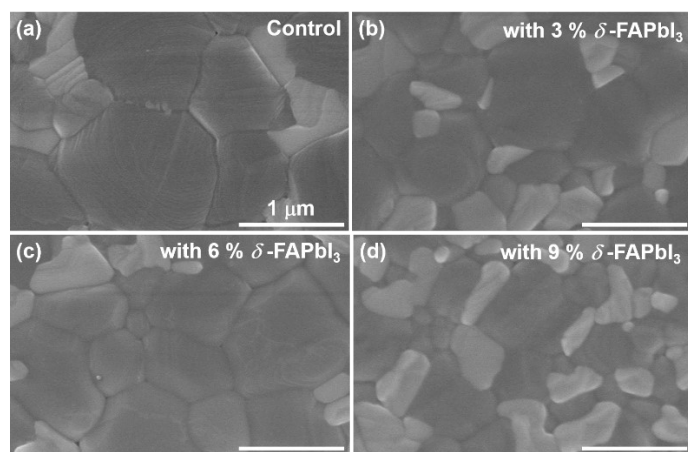


Figure S3. Top-view SEM images of perovskite films with different concentrations of δ -FAPbI₃.

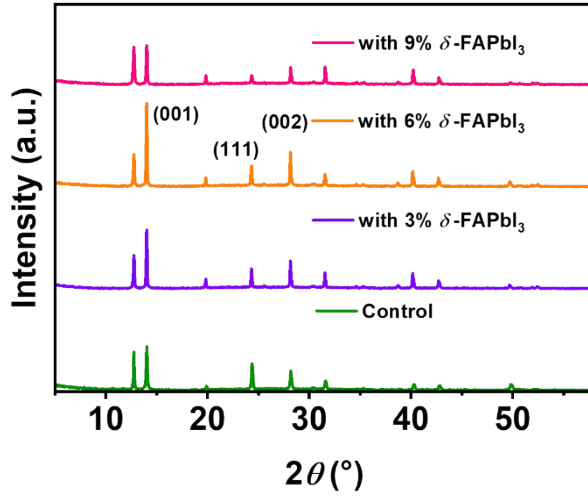


Figure S4. XRD patterns of the perovskite films with different amounts of pre-added δ -FAPbI₃ in the precursors.

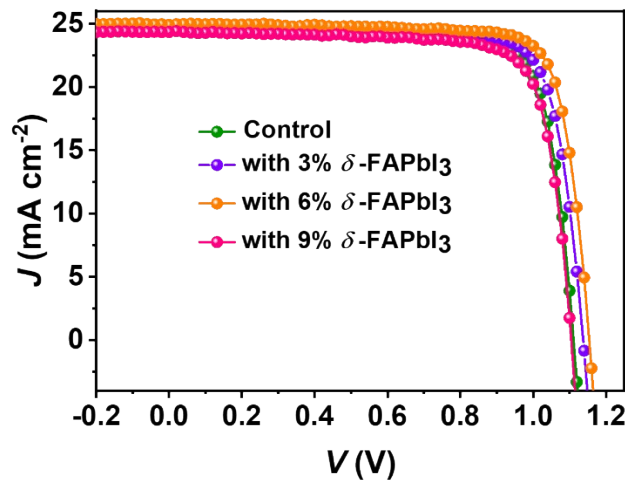


Figure S5. J - V curves of the Pero-SCs with different amounts of pre-added δ -FAPbI₃ in the precursors.

Table S2. Parameters of Pero-SCs based on FA_{1-x}MA_xPbI₃ with varying amounts of δ -FAPbI₃.

Device	V_{OC} (V)	J_{SC} (mA cm ⁻²)	FF (%)	PCE (%)
Control	1.11	24.39	79.6	21.53
With 3% δ -FAPbI ₃	1.13	24.67	79.4	22.23
With 6% δ -FAPbI ₃	1.15	24.94	80.7	23.16
With 9% δ -FAPbI ₃	1.10	24.36	78.3	21.01

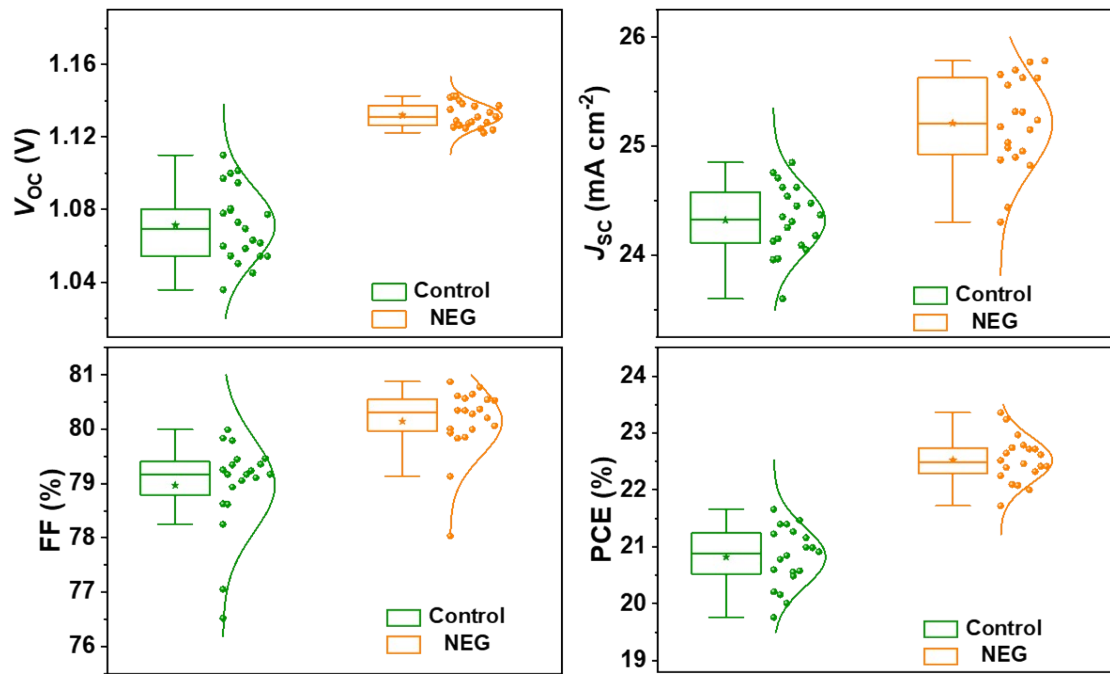


Figure S6. Statistical results of V_{OC} , J_{SC} , PCE and FF based on 20 cells.

Table S3. Photovoltaic parameters of the Pero-SCs under reverse scan (RS) and forward scan (FS) directions.

Device		V_{OC} (V)	J_{SC} (mA cm^{-2})	FF (%)	PCE (%)
Control	FS	1.09	25.59	78.2	21.79
	RS	1.01	25.16	75.5	19.14
NEG	FS	1.16	25.43	78.3	23.20
	RS	1.14	25.03	76.9	22.01

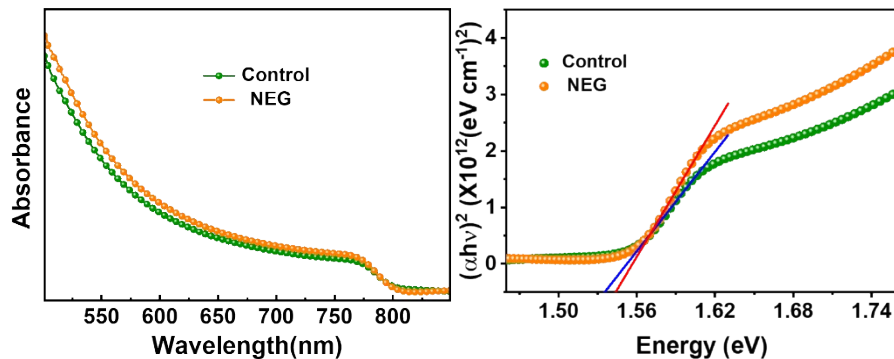


Figure S7. UV-vis spectra and Tauc plots for the control and perovskite films prepared with NEG.

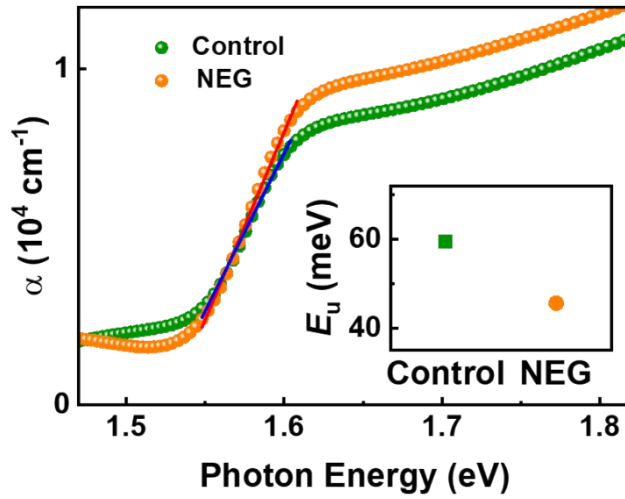


Figure S8. Plots of the absorption coefficient versus the photon energy for the control and perovskite film with NEG. The inset shows an estimated Urbach energy (E_u).

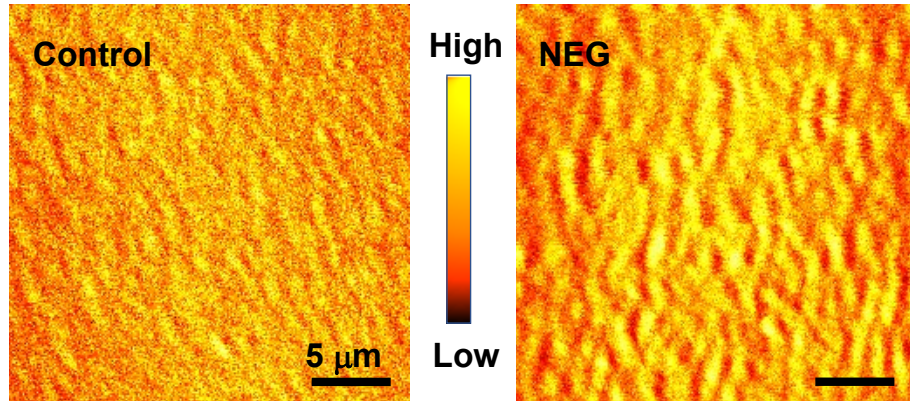


Figure S9. CLSM images of control and perovskite films prepared with NEG.

Table S4. Fitted parameters from TRPL spectra for perovskite films.

Device	τ_1 (ns)	τ_2 (ns)	τ_{ave} (ns)	f_1 (%)	f_2 (%)
Control	21.08	483.32	447.41	7.78	98.22
NEG	35.87	578.54	557.28	3.91	96.09

Table S5. Fitted parameters from ACIS of the Pero-SCs.

Device	R_s (Ω)	R_{tr} (Ω)	C_{tr} (F)	R_{rec} (Ω)	C_{rec} (F)
Control	27.4	67.0	8.0×10^{-9}	1.6	1.6×10^{-6}
NEG	28.0	59.4	9.9×10^{-7}	7.6	7.6×10^{-8}

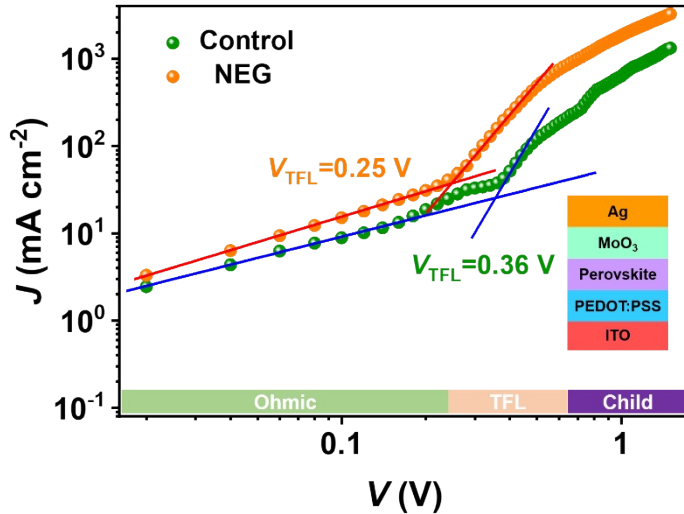


Figure S10. J - V curves measured in the dark of hole-only devices prepared using control and films prepared with NEG for SCLC analysis.

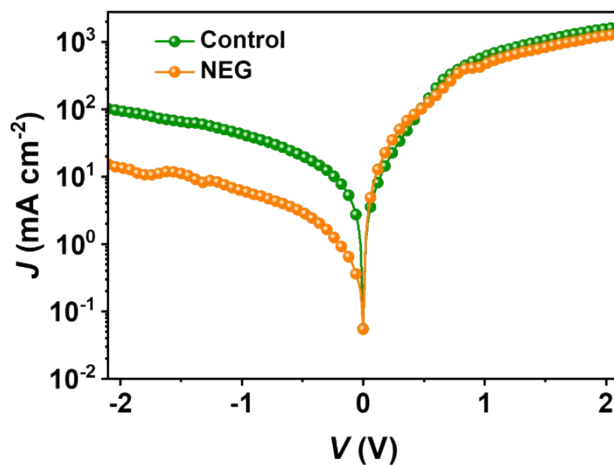


Figure S11. J - V curves of Pero-SCs measured in the dark.

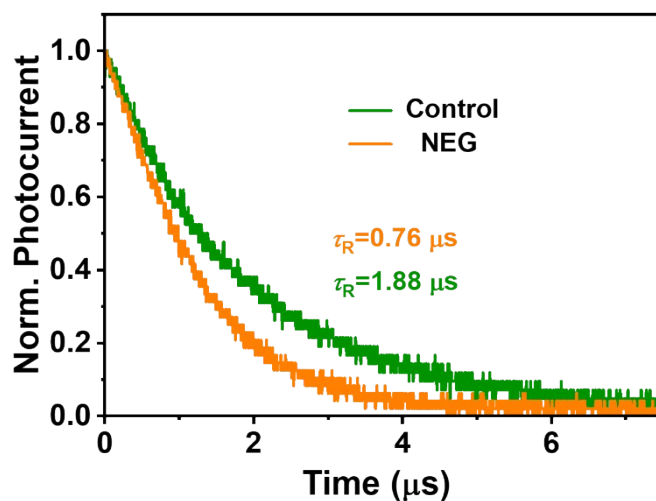


Figure S12. Normalized TPC decay curves of Pero-SCs.

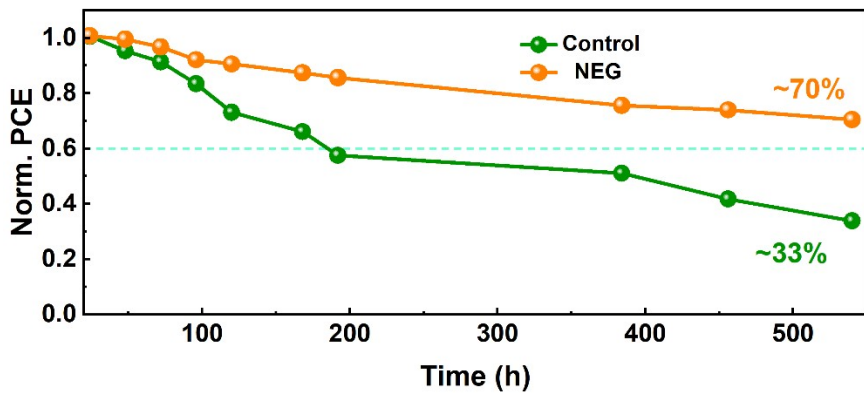


Figure S13. PCE evolution of the unencapsulated devices under 20% RH at 25 °C in the dark.

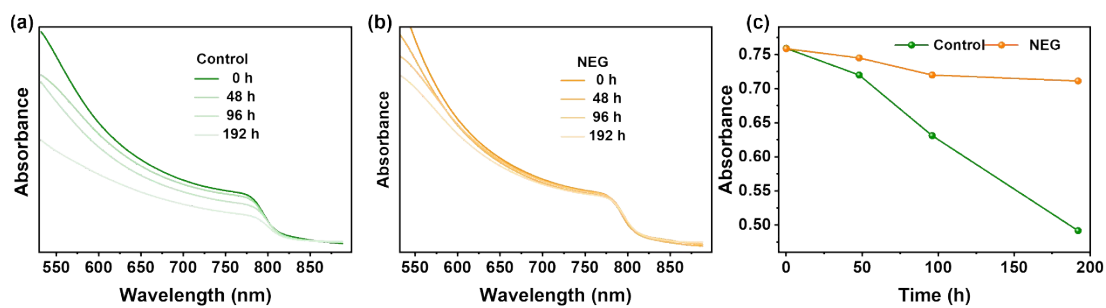


Figure S14. The UV-vis spectra for (a) the control and (b) the perovskite film prepared with NEG at 85 °C in the N₂ glovebox for 192 h, and (c) time dependence curves of the absorbance were monitored at 778 nm for the control film and perovskite film prepared with NEG.

References

1. S. Wang, J. Jin, Y. Qi, P. Liu, Y. Xia, Y. Jiang, R. X. He, B. Chen, Y. Liu and X. Z. Zhao, *Adv. Funct. Mater.*, 2019, **30**, 1908343.
2. E. A. Alharbi, T. P. Baumeler, A. Krishna, A. Y. Alyamani, F. T. Eickemeyer, O. Ouellette, L. Pan, F. S. Alghamdi, Z. Wang, M. H. Alotaibi, B. Yang, M. Almalki, M. D. Mensi, H. Albrithen, A. Albadri, A. Hagfeldt, S. M. Zakeeruddin and M. Grätzel, *Adv. Energy Mater.*, 2021, **11**, 2003785.
3. L. Xie, K. Lin, J. Lu, W. Feng, P. Song, C. Yan, K. Liu, L. Shen, C. Tian and Z. Wei, *J. Am. Chem. Soc.*, 2019, **141**, 20537-20546.
4. F. Qiu, J. Sun, Z. Zhang, T. Shen, H. Liu and J. Qi, *Mater. Today Energy*, 2021, **21**, 100837.
5. Y. Zhao, H. Tan, H. Yuan, Z. Yang, J. Z. Fan, J. Kim, O. Voznyy, X. Gong, L. N. Quan, C. S. Tan, J. Hofkens, D. Yu, Q. Zhao and E. H. Sargent, *Nat. Commun.*, 2018, **9**, 1607.
6. C. Luo, G. Zheng, F. Gao, X. Wang, Y. Zhao, X. Gao and Q. Zhao, *Joule*, 2022, **6**, 240-257.